

IceCube PeV Neutrino Events from the Decay of Superheavy Dark Matter; an Analysis

Madhurima Pandey^{a 1}, Debasish Majumdar^{a 2},

^a*Astroparticle Physics and Cosmology Division,
Saha Institute of Nuclear Physics, HBNI
1/AF Bidhannagar, Kolkata 700064, India*

Ashadul Halder^{b 3}

^b*Department of Physics, St. Xavier's College,
30, Mother Teresa Sarani, Kolkata - 700016, India*

Abstract

Considering the ultrahigh energy (UHE) neutrino events reported by IceCube in the PeV regime to have originated from the decay of superheavy dark matter, the IceCube UHE neutrino events are analysed and the best fit values of the two parameters namely the mass of the superheavy dark matter and its decay lifetime are obtained. The theoretical astrophysical flux is also included in the analysis. We find that while the neutrino events in the energy range ~ 60 TeV- ~ 120 TeV appears to have astrophysical origin, the events in the energy range $\sim 1.2 \times 10^5$ GeV - $\sim 5 \times 10^7$ GeV can be well described from the superheavy dark matter decay hypothesis. We also find that although hadronic decay channel of the superheavy dark matter can well explain the events in the energy range $\sim 1.2 \times 10^5$ GeV - $\sim 5 \times 10^6$ GeV, the higher energy regime higher than this range can be addressed only when the leptonic decay channel is considered.

¹email: madhurima.pandey@saha.ac.in

²email: debasish.majumdar@saha.ac.in

³email: ashadul.halder@gmail.com

1 Introduction

The Icecube (IC) detector at the south pole which uses the southpole ice as the detector material for the neutrinos has so far reported several neutrino events with energies ranging between few hundreds of GeV upto the ultrahigh energy regime of tens of PeV. The events in the TeV-PeV range enables one to probe the neutrinos from extragalactic sources that could produce such high energy neutrinos. This also helps to identify and to ascertain the nature and properties of such possible high energy sources. The event data at IceCube for the neutrino energies greater than 20 TeV are categorized as high energy starting event (HESE) data. The possibility of sources for such data can be of wide range. e.g. Supernova Remnants (SNR) [1], Active Galactic Nuclei (AGN) [2, 3, 4], Gamma Ray Bursts (GRBs) [33] etc. There are also other suggestions in the literature that these UHE neutrinos (in and around PeV region) would have originated from the decay of very heavy dark matter [5]-[29].

In this work we consider the latter possibility mentioned above that the decay of superheavy dark matter (SHDM) could produce the neutrinos detected by the IceCube detector in the energy range ~ 60 TeV- ~ 50 PeV. These SHDMs can produce neutrinos by rare long lived decay processes. They are most likely non-thermal in nature as they could have been created in the early Universe by spontaneous symmetry breaking or through the process of gravitational creation [30, 31]. The IC Collaboration fitted their data of 82 events (HESE data [32]) that include both shower and track events to obtain a power law spectrum for the detected neutrino flux. To this end, they fit first an unbroken power law spectrum of the form $\sim E^{-\gamma}$ where the fitted value of γ is found to be $2.92^{+0.33}_{-0.29}$. The HESE data is referred to the one where the IC Collaboration obtained a flux $\sim E^{-2.9}$ after a single power law fit. But a fit of the data between the energy range ~ 120 TeV to ~ 5 PeV yielded a power law different from the HESE fit ($\gamma \sim 2.9$) indicating the possibility of a second component. This component had been represented as a pink band (specifying 1σ uncertainty) in Fig. 2 of Ref. [32] where IC collaboration furnished their event data for the region(s) now in discussion. Beyond the energy ~ 5 PeV the data points as shown in Fig. 2 of [32] are found to have no lower bound and these data do not appear to follow the fitted spectrum. In this work we consider however the event data points given in Fig. 2 of [32] from ~ 60 TeV upto ~ 50 PeV.

In an earlier work [?], the energy regime only within the pink band has been considered and it has been shown that this part can be well explained by considering a superheavy dark matter decaying to neutrinos only through hadronic channel. In

the present work where we have made a χ^2 analyses for the event data within a larger energy regime of ~ 60 TeV - ~ 50 PeV, we show that in order to explain the apparent nature of the flux beyond ~ 5 PeV one needs to include superheavy dark matter decay through leptonic channel. We also demonstrate that the two event data points in the energy range ~ 60 TeV - ~ 120 TeV in Fig 2 of [32], can be best explained if these two are considered to have astrophysical origin. Our analysis of the whole range of events (from ~ 60 TeV to ~ 50 PeV) suggests that this range seems to have three parts in terms of the possible origins of neutrino events. The energy range spanning between ~ 60 TeV - ~ 120 TeV containing two event data points is the astrophysical component and both the second and third components could have originated from the decay of SHDM. Among the latter two components the event data ranging between $\sim 1.2 \times 10^5$ GeV - $\sim 5 \times 10^6$ GeV are from the hadronic cascade decay of SHDM while the event range $\sim 5 \times 10^6$ GeV - $\sim 5 \times 10^7$ GeV are from the leptonic decay channel of the same SHDM.

In the present analysis, besides incorporating the possible astrophysical origin of neutrinos (diffuse flux), both the hadronic and leptonic channels of the decay cascade of these SHDMs that finally produce the UHE neutrinos are included along with the oscillations/suppressions that the neutrinos of a certain flavour would suffer while traversing the astronomical distance to reach the Earth. We consider three active flavour neutrinos as also the four (3+1) neutrino scheme, where a sterile neutrino is added to the usual three flavour scenario and compare our results. But we find no significant change in results with those obtained for usual 3-flavour case.

The study of the IceCube data [32] in this regime shows that there are two points at energies ~ 60 TeV - ~ 120 TeV and eight number of points are in the energy regime greater than ~ 120 TeV. Among the latter data set three data points do not have any experimental lower limit. The first two data are supposed to be of astrophysical origin [34]. From the analysis presented in this work, it appears that the SHDM decay considerations for UHE neutrino production is most relevant for the neutrinos with energies > 120 TeV ([32]).

The whole set is then fitted with the corresponding data points given by IceCube Collaboration to obtain From the χ^2 analysis presented in this work, the best fit values of the mass of the SHDM and its decay lifetime are also obtained.

The paper is organised as follows. In Section. 2 we briefly describe the superheavy dark matter decay process for both hadronic and leptonic decay channels. UHE neutrino flux in Section. 3 has two subsections. In Subsection. 3.1 we consider the neutrino fluxes from the astrophysical sources while Subsection 3.2 contains the

UHE neutrino fluxes originated from the superheavy dark matter decay. Section. 4 deals with the modified UHE neutrino fluxes at the Earth for both 3-flavour and 4-flavour framework. The calculational results are discussed in Section. 5. Finally, we summarise the paper in Section. 6.

2 Superheavy Dark Matter Decays

The decay of superheavy dark matter particles (SHDMs) that could be produced in the early Universe proceed via the cascading of QCD partons. For the case of the decay of SHDM particles with masses m_χ much larger than the electroweak scale $m_\chi \gg m_W$, the electroweak cascade occurs in addition to the QCD cascade [35, 36]. The production mechanism of the hadronic QCD spectrum including supersymmetric QCD cascade depends on two different methods. One of these two most effective methods is the Monte Carlo (MC) simulation [37, 38] while the other one is the Dokshitzer-Gribov-Lipatov-Altarelli-Parisi (DGLAP) equation [38]-[42], which describes the evolution of the fragmentation function. We obtain the neutrino spectrum/flux as the final product of the numerical evolution of the DGLAP equations and the MC studies and this spectrum/flux is used in this work to explain the IceCube events in ultrahigh energy regime. The whole process of the production of neutrino spectrum can be described by the two decay channels namely, the hadronic and the leptonic decay channels.

2.1 Hadronic Decay Channels of SHDM

QCD cascade from the decay of superheavy particles plays a significant role to describe the production of hadrons. It is asserted that even though the QCD coupling is small, the cascading in QCD parton appears due to the enhancement of the parton splitting in the presence of large logarithms for soft parton emission. The electroweak radiative corrections can also be dominated by similar logarithms. In the case of QCD cascade, we use the numerical code [38] for the evolution of the DGLAP equations. A similar kind of approach can be adopted by the electroweak radiative corrections at the TeV energy scale or above [43]-[48] valid for spontaneously broken gauge group. In this section, we discuss in particular the hadronic decay channel $\chi \rightarrow q\bar{q}$, where q indicates a quark with a flavour. In this decay channel, after the perturbative evolution of the QCD cascade, the partons are hadronized and finally, as the end product, the leptons are obtained by the subsequent decay of the unstable hadrons. In comparison to the

other theoretical uncertainties the effect of electroweak radiative corrections on the cascade development are insignificant.

The neutrino spectrum can be written as [49]

$$\frac{dN_\nu}{dx} = 2R \int_{xR}^1 \frac{dy}{y} D^{\pi^\pm}(y) + 2 \int_x^1 \frac{dz}{z} f_{\nu_i}\left(\frac{y}{z}\right) D_i^{\pi^\pm}(z), \quad (1)$$

where $D_i^\pi(x, s)$ ($\equiv [D_q^\pi(x, s) + D_g^\pi(x, s)]$) is a fragmentation function of the pions from a parton i ($= q(= u, d, s, \dots), g$). The total decay spectrum $F^h(x, s)$ can be obtained by the summation of the contributions of all possible parton (quarks, antiquarks and gluons) fragmentation functions ($D_i^\pi(x, s)$), where x ($\equiv 2E/m_\chi$), a dimensionless quantity, defines the fraction of energy transferred to the hadron and \sqrt{s} is the centre of mass energy. In our calculation we consider only the contribution of pion decays and the contribution ($\sim 10\%$) from other mesons are neglected following Ref. [38]. In Eq. (1), $R = \frac{1}{1-r}$, where $r = (m_\mu/m_\pi)^2 \simeq 0.573$ and the functions $f_{\nu_i}(x)$ are given as [50]

$$\begin{aligned} f_{\nu_i}(x) &= g_{\nu_i}(x)\Theta(x-r) + (h_{\nu_i}^{(1)}(x) + h_{\nu_i}^{(2)}(x))\Theta(r-x), \\ g_{\nu_\mu}(x) &= \frac{3-2r}{9(1-r)^2}(9x^2 - 6\ln x - 4x^3 - 5), \\ h_{\nu_\mu}^{(1)}(x) &= \frac{3-2r}{9(1-r)^2}(9r^2 - 6\ln r - 4r^3 - 5), \\ h_{\nu_\mu}^{(2)}(x) &= \frac{(1+2r)(r-x)}{9r^2}[9(r+x) - 4(r^2 + rx + x^2)], \\ g_{\nu_e}(x) &= \frac{2}{3(1-r)^2}[(1-x)(6(1-x)^2 + r(5+5x-4x^2)) + 6r\ln x] \\ h_{\nu_e}^{(1)}(x) &= \frac{2}{3(1-r)^2}[(1-r)(6-7r+11r^2-4r^3) + 6r\ln r], \\ h_{\nu_e}^{(2)}(x) &= \frac{2(r-x)}{3r^2}(7r^2 - 4r^3 + 7xr - 4xr^2 - 2x^2 - 4x^2r). \end{aligned} \quad (2)$$

2.2 Leptonic Decay Channels of SHDM

The development of electroweak cascade can be illustrated by considering a tree level decay of superheavy particle χ with mass $m_\chi \leq m_{\text{GUT}}$ to leptons. According to the Z -burst model, χ particles are decaying into $\bar{l}l$ pairs and $\chi \rightarrow \bar{\nu}\nu$ is the corresponding decay mode. For $m_\chi \gg m_z$ (m_z being the z boson mass), considering the available momentum flow, ($Q^2 \leq \frac{m_\chi^2}{4}$) we can neglect the mass of the Z boson. The smallness of the QCD coupling can be compensated by a very large logarithms $\ln^2(m_\chi^2/m_z^2)$,

which is generated for soft or collinear singularities. Similarly for $m_\chi \gg m_W$ (m_W being the mass of W boson), due to large logarithms the perturbation theory is no more valid and this initiates developing of the electroweak cascade, very similar to that for known QCD cascade. There can be a mutual transmutation of electroweak and QCD cascades because the electroweak gauge bosons also split into quarks. This will modify the hadronic spectra to a limited extent while on the other hand the splitting like $W \rightarrow \bar{\nu}\nu$ contributes to the electroweak part of the cascade. In order to explain the effects of the SHDM particles decaying into the neutrinos as the final product via the leptonic decay channels, the MC simulations for both the QCD part [37] and the electroweak cascade [51] have been performed.

3 Ultrahigh Energy Neutrino Flux

In this work, we consider the neutrino flux with energies above ~ 60 TeV. The present analysis has been performed for the high energetic IceCube events by considering two different components of the neutrino flux, namely the astrophysical neutrino flux and the neutrino flux from the SHDM decay.

3.1 Astrophysical Neutrino Flux

Numerous astrophysical sources can produce high energy neutrinos through their highly energetic particle acceleration mechanism of protons, where the latter interact with themselves (pp interactions) or with photons ($p\gamma$ interactions) to finally produce neutrinos. Distant ultrahigh energy (UHE) sources like extragalactic Supernova Remnants (SNR) [1], Active Galactic Nuclei (AGN) [2, 3, 4], Gamma Ray Bursts (GRBs) [33] etc. are proposed as the source of IceCube neutrino induced muon events in UHE regime. In the particle acceleration process, a high energetic shock wave generates and progresses outwards with energies as high as $\sim 10^{53}$ ergs in the form of fireball. The interactions between the protons and the photons inside such a fireball produce pions, while these pions decay to finally produce UHE neutrinos. In this work, we consider the contribution of the astrophysical neutrino flux as the source neutrino flux in the ~ 60 - ~ 120 TeV energy range.

In order to consider the acceleration mechanism related to the astrophysical sources, the isotropic fluxes for the neutrinos are estimated by an Unbroken Power Law (UPL)

after summing over all the possible sources and is given as [34]

$$E_\nu^2 \frac{d\phi'_{\nu_{Ast}}}{dE_\nu}(E_\nu) = N \left(\frac{E_\nu}{100 \text{TeV}} \right)^{-\gamma} \text{ GeV cm}^{-2} \text{ s}^{-1} \text{ sr}^{-1}, \quad (3)$$

where N represents the normalization factor of the flux and γ is the spectral index. We have chosen the values of N and γ for our analyses as 1×10^{-8} and 1.0 respectively for UPL [34]. Assuming the neutrinos are produced in the flavour ratio 1:2:0, the flux for ν_e in this case at source will be $\frac{1}{3} \frac{d\phi'_{\nu_{Ast}}}{dE_\nu} = \frac{d\phi_{\nu_{Ast}}}{dE_\nu}$.

Here we mention that for the astrophysical flux we also adopt the power law spectrum given by IceCube Collaboration in Ref. [32] (Fig. 2 of [32]). This is of the form

$$E_\nu^2 \frac{d\phi}{dE_\nu}(E_\nu) = 2.46 \pm 0.8 \times 10^{-8} (E/100 \text{TeV})^{-0.92} \text{ GeV cm}^{-2} \text{ s}^{-1} \text{ sr}^{-1}. \quad (4)$$

Thus our analysis is done for each of the both astrophysical fluxes given here.

3.2 Neutrino Flux from Superheavy Dark Matter Decay

The neutrino flux from superheavy dark matter decay has two components namely a galactic component and the other an extragalactic component. The galactic neutrino flux from the decay of superheavy dark matter with mass m_χ and decay lifetime τ can be written as

$$\frac{d\Phi_G}{dE_\nu}(E_\nu) = \frac{1}{4\pi m_\chi \tau} \int_V \frac{\rho_\chi(R[r])}{4\pi r^2} \frac{dN}{dE}(E, l, b) dV, \quad (5)$$

where the neutrino spectrum from decaying superheavy dark matter particle is defined as $\frac{dN}{dE}(E, l, b)$, l and b are the galactic coordinates. In the above, $\rho_\chi(R[r])$ is the dark matter density, which is a function of the distance (R) from the Galactic Center and r indicates the distance from the Earth. We adopt the Navarro-Frenk-White (NFW) profile for the dark matter density [52, 53] in this work. The integration is made over the Milky Way halo for which the maximum value of R is chosen as $R_{\text{max}} = 260 \text{ Kpc}$ [54].

The isotropic extragalactic neutrino flux from similar decay is given as

$$\frac{d\Phi_{EG}}{dE_\nu}(E_\nu) = \frac{1}{4\pi m_\chi \tau} \int_0^\infty \frac{\rho_0 c/H_0}{\sqrt{\Omega_m(1+z^3) + (1-\Omega_m)}} \frac{dN}{dE}[E(1+z)] dz. \quad (6)$$

In the above equation (Eq. (6)), $c/H_0 = 1.37 \times 10^{28} \text{ cm}$ signifies the Hubble radius and $\rho_0 (= 1.15 \times 10^{-6} \text{ GeV/cm}^3)$ is the average cosmological dark matter density

at the redshift $z = 0$ (present epoch). The contribution of the matter density to the energy density of the Universe in units of the critical energy density is defined as $\Omega_m = 0.316$. The injected neutrino energy spectrum obtained from the decay of superheavy particles is denoted as $\frac{dN}{dE_\nu}$, which is a function of the particle energy shift z , $E(z) = (1+z)E$. For both the galactic and extragalactic neutrino fluxes it is assumed that they reach Earth in the ratio 1:1:1 for three neutrino flavours (ν_e, ν_μ, ν_τ). Therefore at source the ν_e flux can be taken to be Eq. (5) and Eq. (6) for galactic and extragalactic cases respectively. This is also to note that each of the fluxes $\frac{d\Phi_{\text{EG}}}{dE}(E_\nu)$ and $\frac{d\Phi_{\text{G}}}{dE}(E_\nu)$ in fact has two components namely the one that is of hadronic origin and the other which is obtained from leptonic decay channel. Therefore $\frac{d\Phi_{\text{EG}}}{dE}(E_\nu) = \left(\frac{d\Phi_{\text{EG}}}{dE}(E_\nu)\right)_{\text{had}} + \left(\frac{d\Phi_{\text{EG}}}{dE}(E_\nu)\right)_{\text{lep}}$ and $\frac{d\Phi_{\text{G}}}{dE}(E_\nu) = \left(\frac{d\Phi_{\text{G}}}{dE}(E_\nu)\right)_{\text{had}} + \left(\frac{d\Phi_{\text{G}}}{dE}(E_\nu)\right)_{\text{lep}}$.

Thus the total electron neutrino flux at the source, (diffuse astrophysical sources and the decay of superheavy dark matter), can be written as

$$\begin{aligned} \phi^{\text{th}}(E_\nu) = & \frac{d\phi_{\nu_{\text{Ast}}}}{dE_\nu}(E_\nu) + \left(\frac{d\Phi_{\text{EG}}}{dE}(E_\nu)\right)_{\text{had}} + \left(\frac{d\Phi_{\text{G}}}{dE}(E_\nu)\right)_{\text{had}} + \left(\frac{d\Phi_{\text{EG}}}{dE}(E_\nu)\right)_{\text{lep}} + \\ & \left(\frac{d\Phi_{\text{G}}}{dE}(E_\nu)\right)_{\text{lep}}, \end{aligned} \quad (7)$$

where for the first term on the R.H.S., two analytical forms are adopted as discussed in Sect. 3.1.

4 Neutrino Oscillations and the Modified Flux

A neutrino $|\nu_\alpha\rangle$ of flavour α can oscillate to a neutrino $|\nu_\beta\rangle$ with flavour β after traversing a baseline length of L and the oscillation probability can be written as [55]

$$P_{\nu_\alpha \rightarrow \nu_\beta} = \delta_{\alpha\beta} - 4 \sum_{j>i} U_{\alpha i} U_{\beta i} U_{\alpha j} U_{\beta j} \sin^2 \left(\frac{\pi L}{\lambda_{ij}} \right), \quad (8)$$

where i, j indicate the mass indices and $U_{\alpha i}$ etc. denote the neutrino mass-flavour mixing matrix elements (Pontecorvo-Maki-Nakagawa-Sakata (PMNS) matrix) [56]. The flavour eigenstate $|\nu_\alpha\rangle$ relates to the mass eigenstate $|\nu_i\rangle$ through the relation

$$|\nu_\alpha\rangle = \sum_i U_{\alpha i} |\nu_i\rangle, \quad (9)$$

The oscillation length, which is mentioned in Eq. (8), is given by

$$\lambda_{ij} = 2.47 \text{ Km} \left(\frac{E}{\text{GeV}} \right) \left(\frac{\text{eV}^2}{\Delta m_{ij}^2} \right). \quad (10)$$

The oscillatory part of the probability equation (Eq. (8)) is averaged to 1/2 due to the long astronomical baseline distance L for the present context of UHE neutrinos ($\Delta m^2 L/E \gg 1$), where E is the neutrino energy and Δm_{ij}^2 being the mass square difference of two neutrinos with mass eigenstates $|\nu_i\rangle$ and $|\nu_j\rangle$. Therefore,

$$\left\langle \sin^2 \left(\frac{\pi L}{\lambda_{ij}} \right) \right\rangle = \frac{1}{2}. \quad (11)$$

With this, the oscillation probability equation (Eq. (8)) takes the form

$$\begin{aligned} P_{\nu_\alpha \rightarrow \nu_\beta} &= \delta_{\alpha\beta} - 2 \sum_{j>i} U_{\alpha i} U_{\beta i} U_{\alpha j} U_{\beta j} \\ &= \delta_{\alpha\beta} - \sum_i U_{\alpha i} U_{\beta i} \left[\sum_{j \neq i} U_{\alpha j} U_{\beta j} \right] \\ &= \sum_j |U_{\alpha j}|^2 |U_{\beta j}|^2. \end{aligned} \quad (12)$$

In the above we use the unitarity condition

$$\sum_i U_{\alpha i} U_{\beta i} = \delta_{\alpha\beta}. \quad (13)$$

Therefore the flux for each flavour on reaching the Earth can be derived as (with the assumption that neutrinos are produced in the ratio $\nu_e : \nu_\mu : \nu_\tau = 1 : 2 : 0$).

$$\begin{aligned} \begin{pmatrix} F_{\nu_e}^3 \\ F_{\nu_\mu}^3 \\ F_{\nu_\tau}^3 \end{pmatrix} &= \begin{pmatrix} |U_{e1}|^2 & |U_{e2}|^2 & |U_{e3}|^2 \\ |U_{\mu1}|^2 & |U_{\mu2}|^2 & |U_{\mu3}|^2 \\ |U_{\tau1}|^2 & |U_{\tau2}|^2 & |U_{\tau3}|^2 \end{pmatrix} \begin{pmatrix} |U_{e1}|^2 & |U_{\mu1}|^2 & |U_{\tau1}|^2 \\ |U_{e2}|^2 & |U_{\mu2}|^2 & |U_{\tau2}|^2 \\ |U_{e3}|^2 & |U_{\mu3}|^2 & |U_{\tau3}|^2 \end{pmatrix} \\ &\times \begin{pmatrix} 1 \\ 2 \\ 0 \end{pmatrix} \phi_{\nu_e}. \end{aligned} \quad (14)$$

With the unitarity conditions of the PMNS matrix the flux for each flavour on reaching the Earth is finally written as

$$\begin{aligned} F_{\nu_e}^3 &= [|U_{e1}|^2(1 + |U_{\mu1}|^2 - |U_{\tau1}|^2) + |U_{e2}|^2(1 + |U_{\mu2}|^2 - |U_{\tau2}|^2) \\ &\quad + |U_{e3}|^2(1 + |U_{\mu3}|^2 - |U_{\tau3}|^2)] \phi_{\nu_e}, \end{aligned}$$

$$\begin{aligned}
F_{\nu_\mu}^3 &= [|\mathcal{U}_{\mu 1}|^2(1 + |\mathcal{U}_{\mu 1}|^2 - |\mathcal{U}_{\tau 1}|^2) + |\mathcal{U}_{\mu 2}|^2(1 + |\mathcal{U}_{\mu 2}|^2 - |\mathcal{U}_{\tau 2}|^2) \\
&\quad + |\mathcal{U}_{\mu 3}|^2(1 + |\mathcal{U}_{\mu 3}|^2 - |\mathcal{U}_{\tau 3}|^2)]\phi_{\nu_e} , \\
F_{\nu_\tau}^3 &= [|\mathcal{U}_{\tau 1}|^2(1 + |\mathcal{U}_{\mu 1}|^2 - |\mathcal{U}_{\tau 1}|^2) + |\mathcal{U}_{\tau 2}|^2(1 + |\mathcal{U}_{\mu 2}|^2 - |\mathcal{U}_{\tau 2}|^2) \\
&\quad + |\mathcal{U}_{\tau 3}|^2(1 + |\mathcal{U}_{\mu 3}|^2 - |\mathcal{U}_{\tau 3}|^2)]\phi_{\nu_e} .
\end{aligned} \tag{15}$$

Where

$$\mathcal{U} = \begin{pmatrix} c_{12}c_{13} & s_{12}c_{13} & s_{13} \\ -s_{12}c_{23} - c_{12}s_{23}s_{13} & c_{12}c_{23} - s_{12}s_{23}s_{13} & s_{23}c_{13} \\ s_{12}s_{23} - c_{12}c_{23}s_{13} & -c_{12}s_{23} - s_{12}c_{23}s_{13} & c_{23}c_{13} \end{pmatrix} . \tag{16}$$

Proceeding similarly for the 4-flavour oscillation scenario, the flux for each flavour on reaching the Earth is obtained as

$$\begin{aligned}
\begin{pmatrix} F_{\nu_e}^4 \\ F_{\nu_\mu}^4 \\ F_{\nu_\tau}^4 \\ F_{\nu_s}^4 \end{pmatrix} &= \begin{pmatrix} |\tilde{U}_{e1}|^2 & |\tilde{U}_{e2}|^2 & |\tilde{U}_{e3}|^2 & |\tilde{U}_{e4}|^2 \\ |\tilde{U}_{\mu 1}|^2 & |\tilde{U}_{\mu 2}|^2 & |\tilde{U}_{\mu 3}|^2 & |\tilde{U}_{\mu 4}|^2 \\ |\tilde{U}_{\tau 1}|^2 & |\tilde{U}_{\tau 2}|^2 & |\tilde{U}_{\tau 3}|^2 & |\tilde{U}_{\tau 4}|^2 \\ |\tilde{U}_{s1}|^2 & |\tilde{U}_{s2}|^2 & |\tilde{U}_{s3}|^2 & |\tilde{U}_{s4}|^2 \end{pmatrix} \begin{pmatrix} |\tilde{U}_{e1}|^2 & |\tilde{U}_{\mu 1}|^2 & |\tilde{U}_{\tau 1}|^2 & |\tilde{U}_{s1}|^2 \\ |\tilde{U}_{e2}|^2 & |\tilde{U}_{\mu 2}|^2 & |\tilde{U}_{\tau 2}|^2 & |\tilde{U}_{s2}|^2 \\ |\tilde{U}_{e3}|^2 & |\tilde{U}_{\mu 3}|^2 & |\tilde{U}_{\tau 3}|^2 & |\tilde{U}_{s3}|^2 \\ |\tilde{U}_{e4}|^2 & |\tilde{U}_{\mu 4}|^2 & |\tilde{U}_{\tau 4}|^2 & |\tilde{U}_{s4}|^2 \end{pmatrix} \\
&\quad \times \begin{pmatrix} 1 \\ 2 \\ 0 \\ 0 \end{pmatrix} \phi_{\nu_e} .
\end{aligned} \tag{17}$$

Eq. (17) follows that

$$\begin{aligned}
F_{\nu_e}^4 &= [|\tilde{U}_{e1}|^2(1 + |\tilde{U}_{\mu 1}|^2 - |\tilde{U}_{\tau 1}|^2 - |\tilde{U}_{s1}|^2) + |\tilde{U}_{e2}|^2(1 + |\tilde{U}_{\mu 2}|^2 - |\tilde{U}_{\tau 2}|^2 - |\tilde{U}_{s2}|^2) \\
&\quad + |\tilde{U}_{e3}|^2(1 + |\tilde{U}_{\mu 3}|^2 - |\tilde{U}_{\tau 3}|^2 - |\tilde{U}_{s3}|^2) + |\tilde{U}_{e4}|^2(1 + |\tilde{U}_{\mu 4}|^2 - |\tilde{U}_{\tau 4}|^2 - |\tilde{U}_{s4}|^2)]\phi_{\nu_e} , \\
F_{\nu_\mu}^4 &= [|\tilde{U}_{\mu 1}|^2(1 + |\tilde{U}_{\mu 1}|^2 - |\tilde{U}_{\tau 1}|^2 - |\tilde{U}_{s1}|^2) + |\tilde{U}_{\mu 2}|^2(1 + |\tilde{U}_{\mu 2}|^2 - |\tilde{U}_{\tau 2}|^2 - |\tilde{U}_{s2}|^2) \\
&\quad + |\tilde{U}_{\mu 3}|^2(1 + |\tilde{U}_{\mu 3}|^2 - |\tilde{U}_{\tau 3}|^2 - |\tilde{U}_{s3}|^2) + |\tilde{U}_{\mu 4}|^2(1 + |\tilde{U}_{\mu 4}|^2 - |\tilde{U}_{\tau 4}|^2 - |\tilde{U}_{s4}|^2)]\phi_{\nu_e} , \\
F_{\nu_\tau}^4 &= [|\tilde{U}_{\tau 1}|^2(1 + |\tilde{U}_{\mu 1}|^2 - |\tilde{U}_{\tau 1}|^2 - |\tilde{U}_{s1}|^2) + |\tilde{U}_{\tau 2}|^2(1 + |\tilde{U}_{\mu 2}|^2 - |\tilde{U}_{\tau 2}|^2 - |\tilde{U}_{s2}|^2) \\
&\quad + |\tilde{U}_{\tau 3}|^2(1 + |\tilde{U}_{\mu 3}|^2 - |\tilde{U}_{\tau 3}|^2 - |\tilde{U}_{s3}|^2) + |\tilde{U}_{\tau 4}|^2(1 + |\tilde{U}_{\mu 4}|^2 - |\tilde{U}_{\tau 4}|^2 - |\tilde{U}_{s4}|^2)]\phi_{\nu_e} , \\
F_{\nu_s}^4 &= [|\tilde{U}_{s1}|^2(1 + |\tilde{U}_{\mu 1}|^2 - |\tilde{U}_{\tau 1}|^2 - |\tilde{U}_{s1}|^2) + |\tilde{U}_{s2}|^2(1 + |\tilde{U}_{\mu 2}|^2 - |\tilde{U}_{\tau 2}|^2 - |\tilde{U}_{s2}|^2) \\
&\quad + |\tilde{U}_{s3}|^2(1 + |\tilde{U}_{\mu 3}|^2 - |\tilde{U}_{\tau 3}|^2 - |\tilde{U}_{s3}|^2) \\
&\quad + |\tilde{U}_{s4}|^2(1 + |\tilde{U}_{\mu 4}|^2 - |\tilde{U}_{\tau 4}|^2 - |\tilde{U}_{s4}|^2)]\phi_{\nu_e} ,
\end{aligned} \tag{18}$$

where

$$\tilde{U} = \begin{pmatrix} c_{14}\mathcal{U}_{e1} & c_{14}\mathcal{U}_{e2} & c_{14}\mathcal{U}_{e3} & s_{14} \\ -s_{14}s_{24}\mathcal{U}_{e1} + c_{24}\mathcal{U}_{\mu1} & -s_{14}s_{24}\mathcal{U}_{e2} + c_{24}\mathcal{U}_{\mu2} & -s_{14}s_{24}\mathcal{U}_{e3} + c_{24}\mathcal{U}_{\mu3} & c_{14}s_{24} \\ -c_{24}s_{14}s_{34}\mathcal{U}_{e1} & -c_{24}s_{14}s_{34}\mathcal{U}_{e2} & -c_{24}s_{14}s_{34}\mathcal{U}_{e3} & \\ -s_{24}s_{34}\mathcal{U}_{\mu1} & -s_{24}s_{34}\mathcal{U}_{\mu2} & -s_{24}s_{34}\mathcal{U}_{\mu3} & c_{14}c_{24}s_{34} \\ +c_{34}\mathcal{U}_{\tau1} & +c_{34}\mathcal{U}_{\tau2} & +c_{34}\mathcal{U}_{\tau3} & \\ -c_{24}c_{34}s_{14}\mathcal{U}_{e1} & -c_{24}c_{34}s_{14}\mathcal{U}_{e2} & -c_{24}c_{34}s_{14}\mathcal{U}_{e3} & \\ -s_{24}c_{34}\mathcal{U}_{\mu1} & -s_{24}c_{34}\mathcal{U}_{\mu2} & -s_{24}c_{34}\mathcal{U}_{\mu3} & c_{14}c_{24}c_{34} \\ -s_{34}\mathcal{U}_{\tau1} & -s_{34}\mathcal{U}_{\tau2} & -s_{34}\mathcal{U}_{\tau3} & \end{pmatrix} \quad (19)$$

In our calculation, we consider that the intrinsic electron neutrino flux at the source (ϕ_{ν_e}) is equivalent to the theoretical flux $\phi^{\text{th}}(E_\nu)$ (mentioned in the Section 2) obtained from the decay of superheavy dark matter particles. From the above formalism it is evident that the computation of neutrino flux of any flavour on reaching the Earth (after undergoing neutrino oscillation) can be done if ν_e flux at the source can be computed and with the proper evaluation of the PMNS mixing matrix elements.

5 Calculations and Results

We propose in this work that the high energy neutrino events detected by IceCube could have originated from the decay of superheavy dark matter. In case some events might have astrophysical origin, we include in our analyses, this possibility also. By these analyses, we demonstrate that while the two reported events in the energy range ~ 60 TeV - ~ 120 TeV can be best explained when the astrophysical flux is considered in the analysis and the rest can be very well fitted with both the hadronic and leptonic channel production of SHDM decay.

5.1 The choice and data

We have considered the energy region ~ 60 TeV - $\sim 5 \times 10^7$ GeV in our analysis. The event data points as given by IceCube Collaboration (Fig. 2 of Ref. [32]) can be categorized in three regions for three energy ranges. In Fig. 1, we have reproduced, from Fig. 2 of Ref. [32], the energy range (and event data points) from which the data sets for the present analysis has been chosen.

1. Range ~ 60 TeV to ~ 120 TeV

There are two event points in the range ~ 60 TeV- ~ 120 TeV. These two points are adopted in our analysis.

2. Range $\sim 1.2 \times 10^5$ GeV - $\sim 5 \times 10^6$ GeV

There are four data points in the energy region $\sim 1.2 \times 10^5$ GeV to $\sim 5 \times 10^6$ GeV. For one of the four points, only upper limit is given. This region is designated by a pink band (Fig. 2 of Ref. [32] and Fig. 1) and is used for the analysis of the upgoing muon neutrino spectrum in this region. The width of the band indicates 1σ uncertainty. In our analysis (with dark matter decay consideration) we adopt the three points in this region (along with the errors) that is included in the pink band and also choose another 12 points from the pink band with the error given by the width of the band. Thus, in this region we have a total of 15 points.

3. Range $\sim 5 \times 10^6$ GeV - $\sim 5 \times 10^7$ GeV

In this energy range, the IC Collaboration in Fig. 2 of Ref. [32], indicates upper limits of four event points. One may immediately notice that the nature of these four upper bounds grossly differ from that of the pink band. In this work we adopt these upper bounds as event points.

All the 21 event points (henceforth referred to as “data points”) used in the present analyses are enlisted in Table 1.

5.2 Definition of χ^2

We have made χ^2 analyses with data points of the whole range of energies (or for two different ranges together) to understand the role of different components of our proposed dark matter decay origin (through either or both hadronic and leptonic channels) of ultra high energy neutrinos as well as the astrophysical components and for interpreting the events in case of three different regions mentioned above. The parameters in the analysis are the mass of superheavy dark matter m_χ and the decay lifetime τ which are obtained from χ^2 fitting of the data points.

The χ^2 for our analysis is defined as

$$\chi^2 = \sum_{i=1}^n \left(\frac{E_i^2 \phi_i^{\text{th}} - E_i^2 \phi_i^{\text{Ex}}}{(\text{err})_i} \right)^2, \quad (20)$$

where n is the number of data points. Note that $n = 21$ when the whole range of energy is considered, $n = 17$ if only energy ranges 1 and 2 are considered etc. In the above, ϕ_i^{th} designates the theoretical flux. For the total energy range, therefore the total flux is as given in Eq. (7), while in case the analysis is performed with partial energy ranges, relevant fluxes or their sum will be considered. In Eq. (20), ϕ_i^{Ex} denotes the experimental data point at energy E_i with error $(\text{err})_i$.

For the χ^2 fit, the theoretical fluxes for electron neutrinos are then computed using Eqs. (3)-(7). After the neutrinos undergo oscillation on reaching the Earth, the muon neutrino flux on arrival is obtained from Eq. (15) (for 3-flavour case) or Eq. (18) (for 4-flavour case).

5.3 Analysis

Following the formalism described above and Section 3 we make the χ^2 fit by χ^2 minimisation with the data given in Table 1. The use has been made of Eqs. (3) - (19) for computations of theoretical flux components namely astrophysical flux and those predicted from our proposition of the decay of a superheavy dark matter via the hadronic and leptonic channels. From the fit, the best fit values of the two unknown parameters of the formalism namely the mass m_χ and the lifetime τ of the decaying dark matter are obtained. The 1σ , 2σ and 3σ ranges for each of the χ^2 analysis are also computed and furnished along with the study of the quantity of fit for different chosen data sets from Table 1.

We furnish the analyses by considering six different cases. These are given below.

- Case I - All 21 points of the Table 1 is fitted with the theoretical flux at source as in Eq. (7) where astrophysical flux at source computed as in Eq. (3).
- Case II - Same as Case I but for astrophysical source flux computed as in Eq. (4) (the power law spectrum given by IC Collaboration).
- Case III - All 21 points of Table 1. But the theoretical flux is computed without the astrophysical component (only the hadronic and leptonic channel of dark matter decay)

$$\phi^{\text{th}}(E_\nu) = \left(\frac{d\Phi_{\text{EG}}}{dE}(E_\nu) \right)_{\text{had}} + \left(\frac{d\Phi_{\text{G}}}{dE}(E_\nu) \right)_{\text{had}} + \left(\frac{d\Phi_{\text{EG}}}{dE}(E_\nu) \right)_{\text{lep}} + \left(\frac{d\Phi_{\text{G}}}{dE}(E_\nu) \right)_{\text{lep}} .$$

- Case IV- All 21 points of Table 1. Theoretical flux

$$\phi^{\text{th}}(E_\nu) = \frac{d\phi_{\nu_{\text{Ast}}}}{dE_\nu}(E_\nu) + \left(\frac{d\Phi_{\text{EG}}}{dE}(E_\nu) \right)_{\text{had}} + \left(\frac{d\Phi_{\text{G}}}{dE}(E_\nu) \right)_{\text{had}}$$

(no leptonic channel for dark matter decay, the astrophysical flux is from Eq. (3)).

- Case V- The last four points of Table 1 excluded. Total number of points = 17. The theoretical flux is calculated as

$$\phi^{\text{th}}(E_\nu) = \frac{d\phi_{\nu_{\text{Ast}}}}{dE_\nu}(E_\nu) + \left(\frac{d\Phi_{\text{EG}}}{dE}(E_\nu) \right)_{\text{had}} + \left(\frac{d\Phi_{\text{G}}}{dE}(E_\nu) \right)_{\text{had}}$$

(no leptonic decay channel and the theoretical astrophysical flux is from Eq. (3)).

Table 1: The selected data points. see text for details. (The error bars for the last four data points are chosen to be the values of data points itself as there are no lower bounds for those data points)

Energy (in GeV)	Neutrino Flux ($E_\nu^2 \frac{d\Phi}{dE}$) (in GeV cm ⁻² s ⁻¹ sr ⁻¹)	Error
6.13446×10^4 *	2.23637×10^8	2.16107×10^8
1.27832×10^5 *	2.70154×10^8	1.30356×10^8
2.69271×10^5 *	7.66476×10^9	8.5082×10^9
1.19479×10^6 *	5.14335×10^9	7.6982×10^9
2.51676×10^6 *	4.34808×10^9	8.4481×10^9
3.54813×10^6	5.25248×10^9	4.1258×10^9
2.30409×10^6	5.71267×10^9	4.1600×10^9
1.52889×10^6	6.21317×10^9	3.9882×10^9
1.05925×10^6	6.61712×10^9	3.7349×10^9
7.18208×10^5	7.04733×10^9	3.9777×10^9
4.46684×10^5	7.66476×10^9	3.6478×10^9
2.86954×10^5	8.16308×10^9	4.1571×10^9
1.90409×10^5	8.87827×10^9	6.2069×10^9
1.43818×10^5	9.65612×10^9	6.8856×10^9
2.51189×10^6	4.16928×10^9	8.2726×10^9
1.19279×10^6	5.03649×10^9	7.5383×10^9
2.68960×10^5	7.50551×10^9	8.1583×10^9
5.30143×10^6 *	1.55414×10^9	
1.10473×10^7 *	4.08265×10^9	
2.32705×10^7 *	6.08407×10^9	
4.90181×10^7 *	1.05021×10^8	

In Figs. 2 - 6 we show (a) the fluxes calculated with the fitted values using corresponding theoretical flux formula and (b) the m_χ - τ contour plot with 1σ , 2σ and 3σ contours. The best fit values for m_χ and τ are also shown.

- It is shown from Figs. 2 - 3 that the first two points of Table 1 (in the energy range ~ 60 TeV - ~ 120 TeV) cannot be fitted if astrophysical flux is not considered.
- The data points in the energy range ($\sim 1.2 \times 10^5$ GeV - $\sim 5 \times 10^7$ GeV) can be well explained from the consideration that these neutrinos originate from the decay of superheavy dark matter.
- The neutrino events within the energy range $\sim 1.2 \times 10^5$ GeV - $\sim 5 \times 10^6$ GeV (pink band) is very well represented by the neutrinos produced from the SHDM decay via *hadronic channel*.
- Fig. 5(a) and Fig. 6(a) clearly demonstrate that only hadronic channel cannot explain the events beyond the energy $\sim 5 \times 10^6$ GeV - $\sim 5 \times 10^7$ GeV. There are indications from this analysis that the data events in the energy range $\sim 5 \times 10^6$ GeV - $\sim 5 \times 10^7$ GeV can only be represented by the neutrinos from *leptonic channel* of SHDM decay in the present framework.

As mentioned, the best fit values of the parameters m_χ and τ (as well as 1σ , 2σ and 3σ contours) for each of the cases are shown in Fig. 2(b) - 6(b) respectively. These values along with the respective values for χ_{\min}^2 are shown in Table 2.

From the above analyses therefore, it can be stated that the UHE neutrino events reported by IC in the energy range $\sim 1.2 \times 10^5$ GeV to $\sim 5 \times 10^7$ GeV can be well described to have originated from the decay of a supermassive dark matter of mass $\sim 10^8$ GeV and decay time $\sim 10^{29}$ sec.

We also like to state that we repeat the entire analysis with 4-flavour oscillation scenario with no or any significant changes. For this purpose the values of mixing angles are chosen as $\theta_{14} = 3.6^\circ$, $\theta_{24} = 4^\circ$, $\theta_{34} = 18.48^\circ$. These values are within the allowed limits of the analyses of NOvA [59], MINOS [60], Daya Bay [61] neutrino experiments.

In Fig. 7 we furnish a ternary plot showing the flavour ratios of the active neutrinos on reaching the Earth for both the 3-flavour and 4-flavour oscillation cases. The flavour (ν_e, ν_μ, ν_τ) ratio of 1:1:1 for active neutrinos are also shown for comparison. The assumed production ratio of 1:2:0 for the active neutrinos is also furnished. The flavour ratio barely changes when 4-flavour oscillation is considered.

Table 2: Best fit values of m_χ and τ for different cases.

Set	m_χ in GeV	τ in sec	Value of χ_{min}^2
All points, All channels (the astrophysical flux is taken from Eq. (3))	1.5461×10^8	2.2136×10^{29}	3.8744
All points, All channels (the flux adopted from the IC Collaboration (Eq. (4)) as the astrophysical flux)	1.4765×10^8	5.6898×10^{29}	9.5042
All points, Leptonic channel, Hadronic channel	1.5640×10^8	1.6410×10^{29}	9.5208
All points, Hadronic channel (pink band points), Astrophysical flux (Eq. (3))	7.586×10^7	1.603×10^{29}	4.6504
First 5 points, Hadronic channel (pink band points), Astrophysical flux (Eq. (3))	1.2679×10^8	1.5314×10^{29}	1.5301

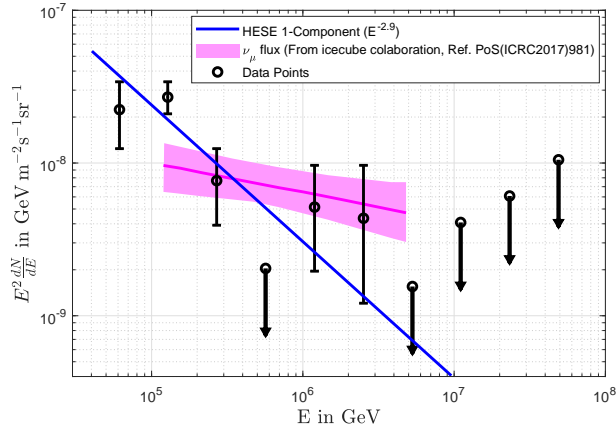


Figure 1: The data points and range of energy considered in the present analyses. The pink band is also shown. These are reproduced from Fig. 2 of Ref. [32]

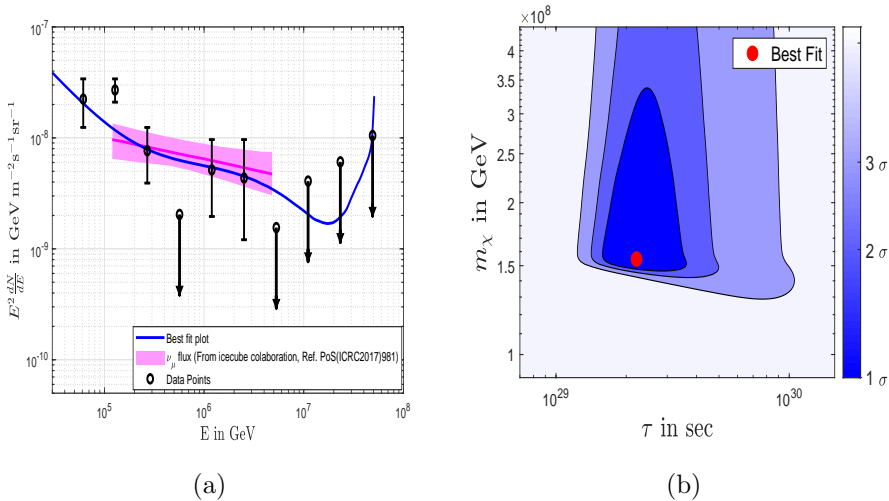


Figure 2: (a) flux, (b) contour by considering all points, all channels (The astrophysical flux is computed from Eq. (3)). See text for details.

6 Discussions and Conclusions

In this work we consider the UHE neutrino events reported by IC Collaboration in the energy range ~ 60 TeV - ~ 50 PeV. We propose that these UHE neutrinos originate from the decay of a supermassive dark matter that could have produced by the process of gravitational production in the early Universe. We make a χ^2 analysis of the IC data in the energy range mentioned above by considering the neutrino flux from such dark matter decay as also from the possible astrophysical origin. For the computation of the astrophysical flux

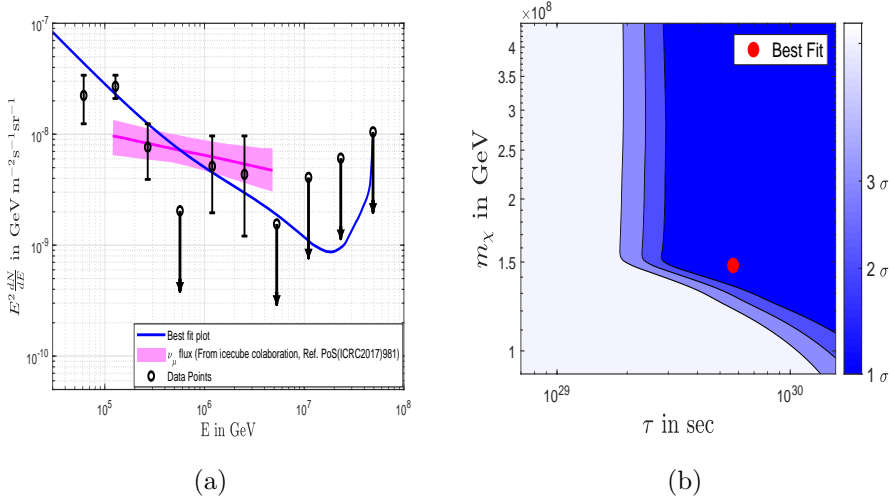


Figure 3: (a) flux, (b) contour by considering all points, all channels (the flux given by the IC Collaboration is considered as the astrophysical flux (Eq. (4))). See text for details.

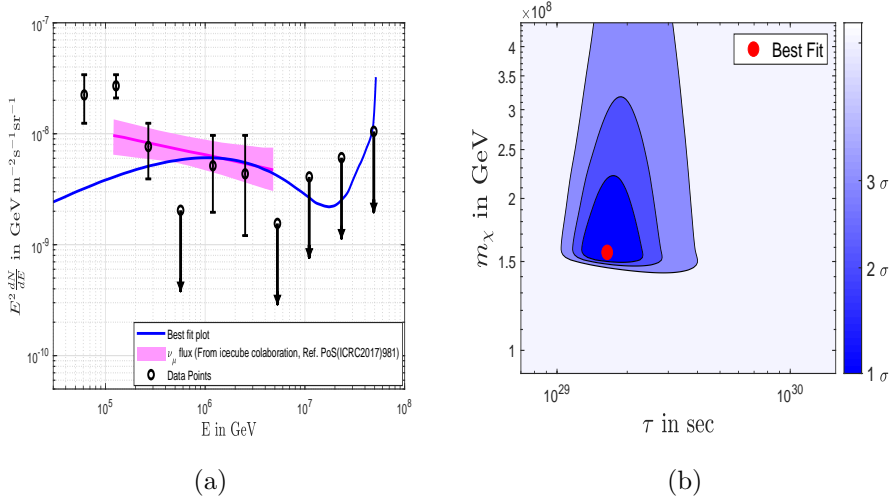


Figure 4: (a) flux, (b) contour by considering all points, lepto-hadronic channels. See text for details.

we consider a Waxman-Bahcall type power law as also the power law $\sim E^{-2.9}$ given by the IC Collaboration from their analysis.

From the present calculations, it appears that the energy range of UHE neutrinos considered here from IC data has three regions. The lower energy range between ~ 60 TeV to ~ 120 TeV represented by two event data points (Fig. 1) appears to be consistent with the flux of astrophysical origin, while for the higher energy range between $\sim 1.2 \times 10^5$ GeV

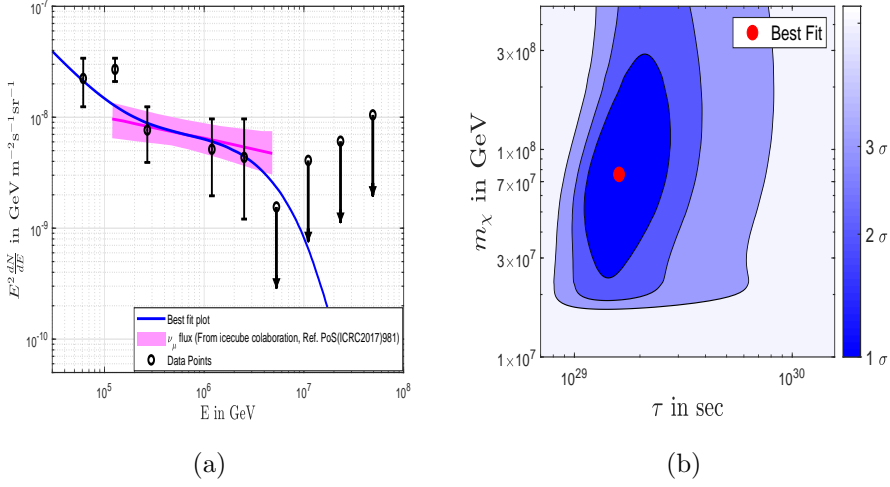


Figure 5: (a)flux, (b) contour by considering all points, hadronic+astro channels (the astrophysical flux is computed from Eq. (3)). See text for details.

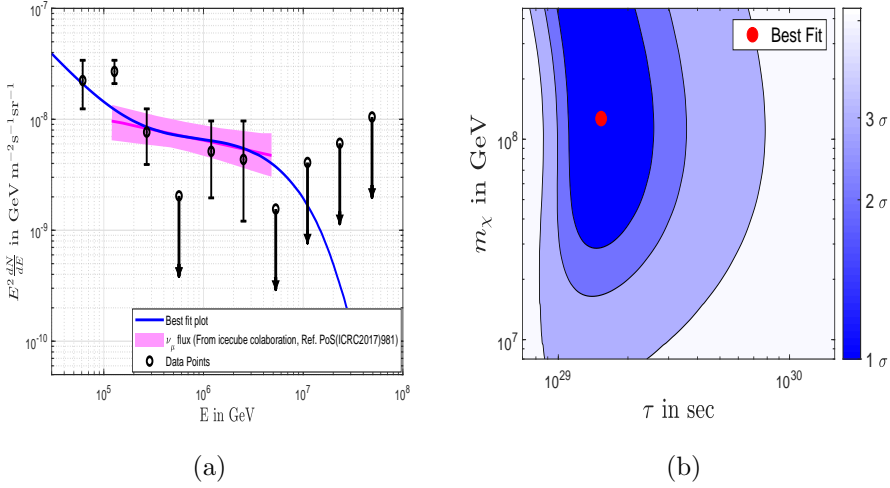


Figure 6: (a)flux, (b) contour by considering first 5 points (except the last three points with large error bar), hadronic+astro channels (Eq. (3) is considered as the astrophysical flux). See text for details.

- $\sim 5 \times 10^7$ GeV, the SHDM decay consideration of neutrino production pursued in this work, appear to describe well. Within this energy range again, the neutrino events in the range between $\sim 1.2 \times 10^5$ GeV - $\sim 5 \times 10^6$ GeV can be very well fitted with the neutrino flux following the hadronic channel of the dark matter decay. This hadronic channel however cannot describe at all the possible events in the higher energy region appearing between $\sim 5 \times 10^6$ GeV - $\sim 5 \times 10^7$ GeV. Although the event data is not very specific in

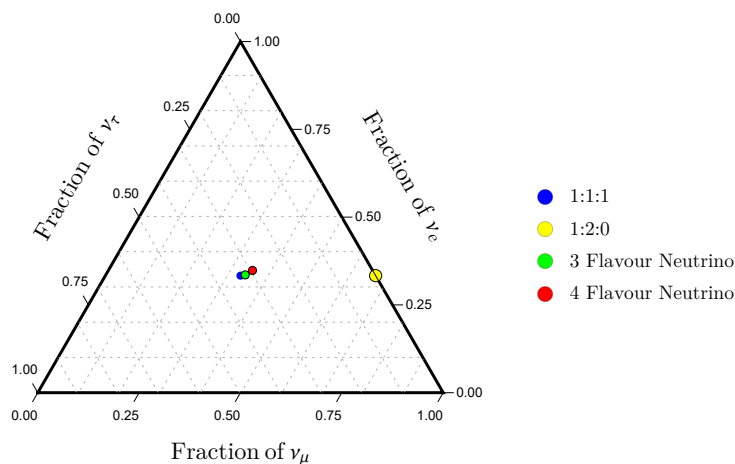


Figure 7: Ternary plot showing the neutrino flavour ratios on arriving the Earth from high energy sources.

this region with only the upper limit of four possible events are given by IC (Fig. 1) but the apparent nature of the flux appears to be very different than what is obtained for the range $\sim 1.2 \times 10^5$ GeV - $\sim 5 \times 10^7$ GeV (well described in this analysis by hadronic channel of SHDM decay). But we find that when the leptonic channel decay of SHDM is included in our analysis, the apparent nature of neutrino flux in this high energy regime can be well represented.

Thus from our analyses it appears that the UHE neutrino signals in the energy range $\sim 1.2 \times 10^5$ GeV - $\sim 5 \times 10^7$ GeV reported by IceCube could have originated from the decay of superheavy dark matter.

Acknowledgments : One of the authors (M.P.) thanks the DST-INSPIRE fellowship (DST/INSPIRE/FELLOWSHIP/IF160004) grant by Department of Science and Technology (DST), Govt. of India. One of the authors (A.H.) wishes to acknowledge the support received from St.Xaviers College, kolkata Central Research Facility and thanks the University Grant Commission (UGC) of the Government of India, for providing financial support, in the form of UGC-CSIR NET-JRF.

References

- [1] S. Chakraborty and I. Izaguirre, Phys. Lett. B **745**, 35 (2015).
- [2] O. Kalashev, D. Semikoz and I. Tkachev, JETP **147**, 3 (2015).
- [3] F.W. Stecker, C. Done, M.H. Slamon, P. Sommers, Phys. Rev. Lett. **66**, 2697 (1991).
- [4] F.W. Stecker, C. Done, M.H. Slamon, P. Sommers, Phys. Rev. Lett. **69**, 2738 (1992).

- [5] A. Anisimov and P. Di Vari, Phys. Rev. D **80**, 073017 (2009).
- [6] J. Zavala, Phys. Rev. D. **89**, 123516 (2014).
- [7] A. Bhattacharya, R. Gandhi and A. Gupta, JCAP **1503**, 027 (2015).
- [8] E. Dudas, Y. Mambrini and K.A. Olive, Phys. Rev. D. **91**, 075001 (2015).
- [9] C. El Aisati, C. Garcia-Cely, T. Hambye and L. Vanderheyden, JCAP **1710**, 021 (2017).
- [10] L. Covi, M. Grefe, A. Ibarra, D. Tran, JCAP **1004**, 017 (2010).
- [11] A. Esmaili, S. K. Kang, P.D. Serpico, JCAP **1412**, 054 (2014).
- [12] C. Rott, K. Kohri, S.C. Park, Phys. Rev. D **92**, 023529 (2015).
- [13] Y. Bai, R. Lu, J. Salvado, JHEP **01**, 161 (2016).
- [14] A. Esmaili, P.D. Serpico, JCAP **1311**, 054 (2013).
- [15] A. Bhattacharya, M.H. Reno, I. Sarcevic, JHEP **06**, 110 (2014).
- [16] A. Esmaili, A. Ibarra, O.L.G. Peres, JCAP **1211**, 034 (2012).
- [17] C.S. Fong, H. Minakata, B. Panes, R.Z. Funchal, JHEP **1502**, 189 (2015).
- [18] C. El Aisati, M. Gustafsson, T. Hambye, Phys. Rev. D **92**, 123515 (2015).
- [19] S.M. Boucenna et al., JCAP **1512**, 055 (2015).
- [20] S. Troitsky, JETP Lett. **102**, 785 (2015).
- [21] M. Chianese, G. Miele, S. Morisi, E. Vitagliano, Phys. Lett. B **757**, 251 (2016).
- [22] M. Chianese, G. Miele, S. Morisi, JCAP **1701**, 007 (2017).
- [23] A. Bhattacharya, A. Esmaili, S. Palomares-Ruiz, I. Sarcevic, JCAP **1707**, 027 (2017).
- [24] M. Chianese, G. Miele, S. Morisi, Phys. Lett. B **773**, 591 (2017).
- [25] M. G. Aartsen *et al.*, IceCube Collaboration, Eur. Phys. J. C **78**, 831 (2018).
- [26] P.S. Bhupal Dev *et al.*, JCAP **1608**, 034 (2016).
- [27] Y. Sui and P.S. Bhupal Dev, JCAP **07**, 020 (2018).
- [28] N. Hiroshima *et al.*, Phys. Rev. D **97**, 023006 (2018).

- [29] V. Brder, J. Kopp and Xiao-Ping Wang, JCAP **01**, 026
- [30] V.A. Kuzmin and I.I. Tkachev, Phys. Rep. **320**, 199 (2019).
- [31] G. Gelmini and P. Gondolo, *Particle Dark Matter; Observations, Models and Searches*, Ed. G. Bertone, Cambridge University Press, Cambridge, U.K. (2010).
- [32] C. Kopper, *Observation of astrophysical neutrinos in six years of IceCube data*, in: Contributed Talk at ICRC 2017 Conference.
- [33] E. Waxman and J.N. Bahcall, Phys. Rev. Lett. **78**, 2292 (1997).
- [34] M. Chianese, J. Phys. Conf. Ser. **718**, 042014 (2016).
- [35] V. Berezhinsky and M. Kachelriess, Phys. Lett. B **422**, 163 (1998).
- [36] V. Berezhinsky and M. Kachelriess, Nucl. Phys. Proc. Suppl. **75**, 377 (1999).
- [37] V. Berezhinsky and M. Kachelriess, Phys. Rev. D **63**, 034007 (2001).
- [38] R. Aloisio, V. Berezhinsky and M. Kachelriess, Phys. Rev. D **69**, 094023 (2004).
- [39] V. Berezhinsky and M. Kachelriess, Phys. Lett. B **434**, 61 (1998).
- [40] S. Sarkar and R. Toldra, Nucl. Phys. B **621**, 495 (2002).
- [41] C. Barbot and M. Drees, Phys. Lett. B **533**, 107 (2002).
- [42] C. Barbot and M. Drees, Astropart. Phys. **20**, 5 (2003).
- [43] P. Ciafaloni and D. Comelli, Phys. Lett. B **446**, 278 (1999).
- [44] M. Beccaria *et al.*, Phys. Rev. D **61**, 073005 (2000).
- [45] V. S. Fadin *et al.*, Phys. Rev. D **61**, 094002 (2000).
- [46] W. Beenakker and A. Werthenbach, Phys. Lett. B **489**, 148 (2000).
- [47] M. Hori, H. Kawamura and J. Kodaira, Phys. Lett. B **491**, 275 (2000).
- [48] A. Denner and S. Pozzorini, Eur. Phys. J. C **18**, 461 (2001).
- [49] M. Kachelriess, O. E. Kalashev and M. Yu. Kuznetsov, Phys. Rev. D. **98**, 083016 (2018).
- [50] S. R. Kelner, F. A. Aharonian and V. V. Bugayov, Phys. Rev. D. **74**, 034018 (2006) [Erratum: Phys. Rev. D. **79**, 039901 (2009)].

- [51] V. Berezhinsky, M. Kachelriess and S. Ostapchenko, Phys. Rev. Lett. **89**, 171802 (2002).
- [52] J.F. Navarro, C.S. Frenk and S.D.M. White. Astrophys. J. **462**, 563 (1996).
- [53] J.F. Navarro, C.S. Frenk and S.D.M. White. Astrophys. J. **490**, 493 (1997).
- [54] M. Cirelli *et al.*, JCAP **1103**, 051 (2011).
- [55] D. Majumdar, A. Ghosal, Phys. Rev. D **75**, 11304 (2007).
- [56] Z. Maki, M. Nakagawa, S. Sakata, Prog. Theo. Phys., **28**, (1962).
- [57] S.K. Kang *et al.* Hinsawi Publishing Corporation **2013**, 138109 (2013).
- [58] H. Athar, M. Jezabek, O. Yasuda, Phys. Rev. D **62**, 103007 (2000).
- [59] D.S. Ayres *et al.* (NOvA Collaboration), arXiv:hep-ex/0503053.
- [60] P. Adamson *et al.* (MINOS Collaboration) Phys. Rev. Lett. **122**, 091803 (2019).
- [61] F.P. An *et al.* (Daya Bay Collaboration), Phys. Rev. Lett. **117**, 151802 (2016).